

STRUCTURE AND PROPERTIES OF NANOCOMPOSITE NICKEL/GRAPHENE OXIDE COATINGS PRODUCED BY ELECTROCHEMICAL REDUCTION METHOD

The paper presents the results of research on nanocomposite nickel/graphene oxide (Ni / GO) coatings produced by electrochemical reduction method on a steel substrate. Discussed is the method of manufacturing composite coatings with nickel matrix and embedded graphene oxide flakes. For comparative purposes, the studies also included a nanocrystalline Ni coating without embedded graphene oxide flakes. Graphene oxide was characterized by Raman spectroscopy, infrared spectroscopy (FTIR) and transmission (TEM) and scanning (SEM) electron microscopy. Results of studies on the structure of nickel and composite Ni/GO coatings deposited in a bath containing different amount of graphene oxide are presented. The coatings were characterized by scanning electron microscopy, light microscopy, Raman spectroscopy and X-ray diffraction. The adhesion of the prepared coatings to the substrate was examined by the scratch method. The microhardness of the coatings was measured using the Vickers method on perpendicular cross-sections to the surface. Corrosion tests of the coatings were investigated using the potentiodynamic method. The influence of graphene oxide on the structure and properties of composite coatings deposited from baths with different content of graphene oxide was determined.

Keywords: graphene oxide, nanocomposites, electrodeposition, nickel/graphene oxide coatings, corrosion tests

1. Introduction

In recent years, metal coatings deposited by electrochemical techniques have become increasingly important. The relatively simple production technology and good usable properties make the so produced coatings as being frequently used in many branches of industries. This method, by controlling the parameters of the deposition process and modification of the production process with the introduction of different phases, makes possible to obtain coatings formed of composite materials with properties much better than those of pure metals. Particularly noteworthy are composite coatings reinforced with carbon materials. The carbon, occurring in many allotropic forms, exhibits unique properties depending on the form in which it is found. In recent decades, various allotropes and forms of carbon have been invented, including fullerenes, carbon nanotubes (CNTs), and graphene. Since the inception of nanotechnology, carbon allotropes-based nanocomposites have become a leading sector of research and advancement due to their unique bonding properties. Current research progress reveals that carbon and its allotropic forms have revolutionized the industry and science community due to their remarkable properties. Important advances in various aspects of allotropic carbon variants and their different applications are reported in

the scientific literature. In particular, carbon allotropic forms are widely used as the dispersion phases being incorporated into coatings produced by chemical and electrochemical reduction methods. The materials produced in this way are characterized by much better mechanical, corrosion and tribological properties, as evidenced by literature reports. In the works [1-3], graphite was used as dispersion phase for producing nanocomposite coatings, while in [4-8] the coating materials were reinforced with diamond nanoparticles. Moreover, studies reported in [9-11] are aimed on the nanocomposite materials with carbon nanotubes as the dispersion phase. Recently, a great deal of interest is focused on the two-dimensional form of the carbon, i.e. on the graphene as a dispersion phase in the composite material [12-18].

The research carried out within this work is aimed on nanocomposite nickel/graphene oxide coatings produced by electrochemical reduction method. The aim of the study was to identify the influence of the content of graphene flakes dispersed in the bath on the structure and selected properties of Ni/GO composite coatings. Two variants of composite coatings with a nickel matrix and graphene oxide as a dispersive phase and, for comparison purpose, a pure nickel coating were produced. The performed investigations attest that such composite coatings can be a promising alternative to currently used coatings.

* LUKASIEWICZ RESEARCH NETWORK – INSTITUTE OF PRECISION MECHANICS, 3 DUCHNICKA STR., 01-796 WARSZAWA, POLAND

Corresponding author: grzegorz.cieslak@imp.edu.pl

2. Experimental

In the present study an attempt was made to produce the nickel coating and nickel/graphene oxide composite coatings by electrochemical reduction method on a DC01 carbon steel substrate. The processes of the deposition of coatings were carried out with multi-component Watts solutions containing: nickel sulphate (source of Ni^{2+} ions), nickel chloride (improvement of bath conductivity), boric acid (pH buffer), sodium dodecyl sulfate (surfactant), saccharin (a brightening agent) and in the case of composite coatings, an aqueous suspension of graphene oxide flakes. The Watts bath has been used because it is characterized by high efficiency and stable work [19-20]. Saccharin, as an additive to the bath, influences the fragmentation of the structure of the coatings [21]. All reagents used were of high purity and were produced by Chempur (Poland). The aqueous GO suspension produced by Graphene Supermarket (USA) was used. Prior to the deposition process, the steel substrate was polished mechanically, degreased with Viennese lime, and digested with 15% H_2SO_4 to ensure good adhesion of the coatings to the substrate. The electrodeposition process of Ni and Ni/GO coatings was carried out at a constant current density of 3 A/dm^2 in the Watts bath at temperature of 318 K and stirred with a magnetic stirrer at 300 rpm. Two variants of Ni/GO composite coatings were obtained from baths with various contents of an aqueous suspension of the graphene oxide (1 and 2 g/dm^3). The graphene oxide used to make nanocomposite deposits was characterized by Raman spectrometry using Renishaw equipment with a green laser with a wavelength of 532 nm, transmission (TEM) and scanning (SEM) electron microscopy and infrared spectroscopy (FTIR). The Ni and Ni/GO coatings were tested using SEM, light microscopy with the Keyence VHX 5000 digital equipment, XRD and Raman spectroscopy. The crystallite size of the nickel matrix material was determined from the diffraction spectrum using the Scherrer's formula [13]. Evaluation of the internal structure of the coatings and Vickers microhardness measurements at 25 G load were made on cross sections perpendicular to the surface by Wilson Hardness T1202 (Buehler) device. Corrosion tests were carried out by electrochemical potentiodynamic

method in a 0.5 M sodium chloride solution at the temperature of $297 \text{ K} \pm 2 \text{ K}$ using the SP-200 potentiostat (Bio-Logic). The measurements were carried out in a three-electrode system with $\text{Hg/Hg}_2\text{Cl}_2/\text{KCl}$ calomel electrode as a reference electrode, the platinum as a counter electrode, and the studied sample (1 cm^2 of exposed surface) as the working electrode. Polarization tests were performed in the range of potentials from -250 mV to 250 mV with respect to the stationary potential. Scanning rate was fixed at 0.2 mVs^{-1} . The extrapolation tangent line to polarization $E = f(j)$ curve from the cathode and anode areas was used to determine the corrosion current density (j_{corr}) and corrosion potential (E_{corr}). Images of corrosion damages were obtained by the Keyence VHX 5000 digital microscope. The adhesion of the coatings to the substrate was examined by the scratching method with a CSM device. A Rockwell type indenter with a progressively varying load in the range $0 \div 100 \text{ N}$ was used with the feed rate of the indenter 10 mm/min. , the scratch length was 10 mm .

3. Results and discussion

3.1. Graphene oxide

For production of nickel/graphene oxide composite coatings were used graphene oxide flakes in the form of an aqueous brown suspension. According to the manufacturer's description [22], the concentration of GO in the suspension was 500 mg/l , carbon content 79 wt% and oxygen 20 wt%. Figures 1-3 show the results of the GO study carried out using SEM and TEM microscopy as well as the Raman and the FTIR spectrometry.

The scanning and transmission electron microscopy observations have shown that the graphene oxide exhibits the form of flakes of various shapes and sizes of the order $1 \mu\text{m}$. On the Raman spectrum, the D (1350 cm^{-1}) and G (1585 cm^{-1}) peaks being characteristic for the graphene oxide can be observed. The peak D characterizes the occurrence of defects in the material and the peak G results from the sp^2 hybridized bonds

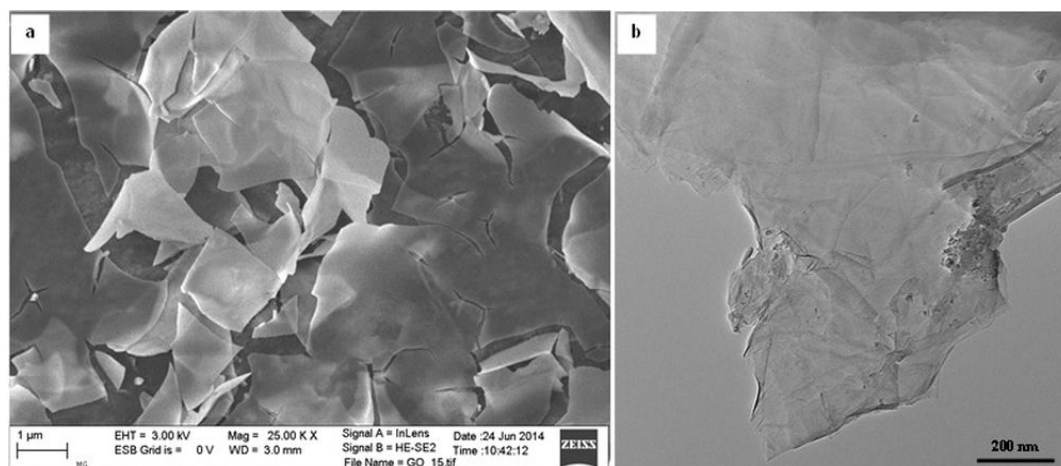


Fig. 1. Graphene oxide: a) SEM image, b) TEM image

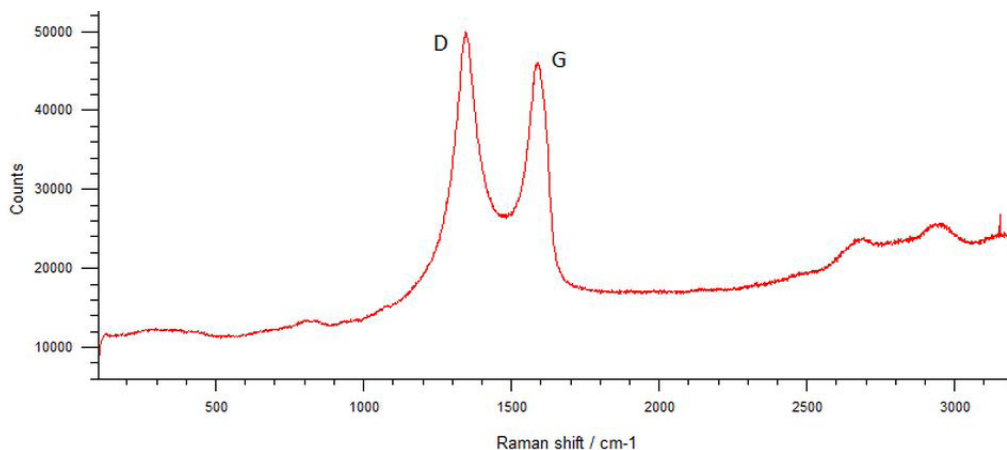


Fig. 2. Raman spectrum of the graphene oxide

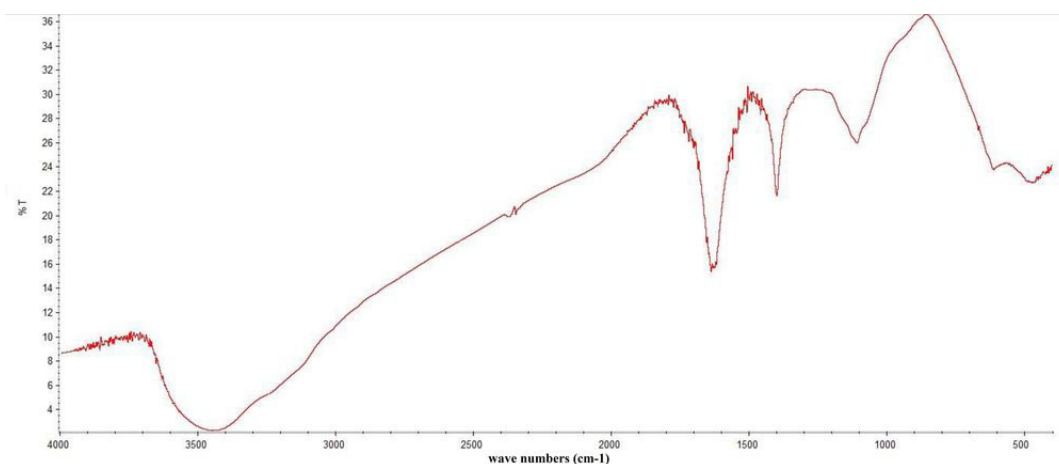


Fig. 3. FTIR spectrum of the graphene oxide

in the material [23]. As is well known the I_D/I_G intensity ratio determines the degree of structure ordering in the material and for the ratio $I_D/I_G > 1$ the material is highly disordered [24]. For the graphene oxide used in the performed studies the determined ratio equals $I_D/I_G = 1.18$ which indicates the high disorder in the studied material. FTIR spectrum of GO shows characteristic IR vibrational infrared bands for groups: OH around 3400 cm⁻¹, C = C ring stretching at 1620 cm⁻¹, phenolic OH deformation near 1412 cm⁻¹ and CO stretching around 1100 cm⁻¹ [17].

3.2. Characteristics of the structure of produced coatings

The images of the surface and cross-section as well as the X-ray diffraction spectrum of the nickel coating produced by electrochemical reduction are shown in Figure 4 and 5.

The Ni coating produced by the electrochemical reduction method is smooth and shiny. The surface morphology is characteristic of coatings deposited from baths containing sac-

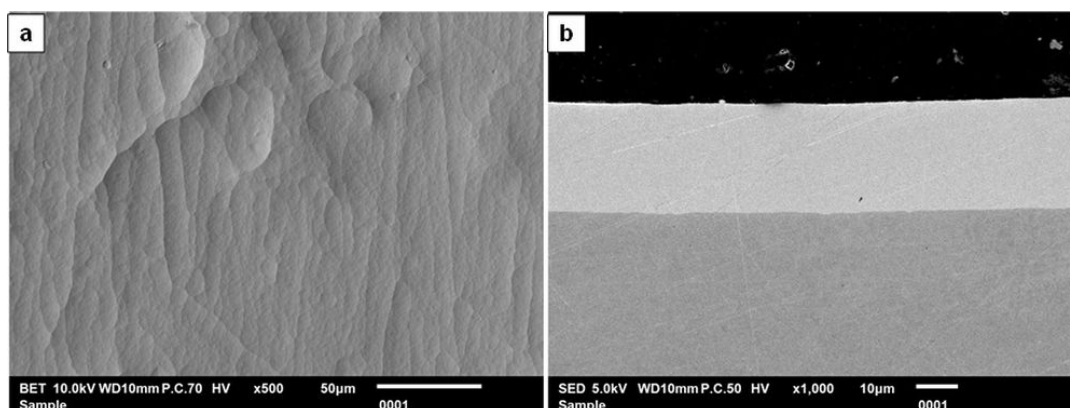


Fig. 4. Surface morphology (a) and cross-section (b) of Ni coating

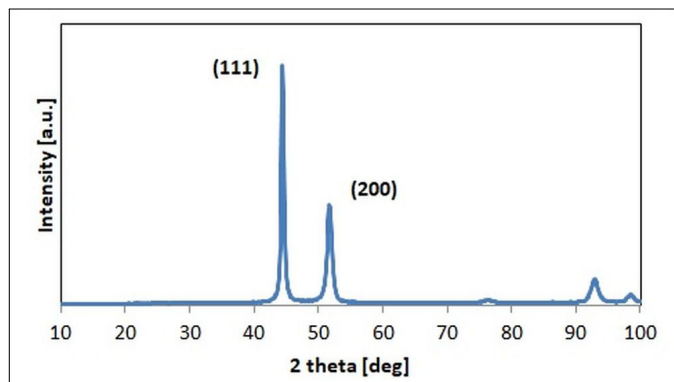


Fig. 5. Diffraction pattern of Ni coating

charin [21,25]. This coating has a compact structure and uniform thickness of about 30 μm . On the diffraction spectrum there are only nickel reflections of varying intensity. The coating has a polycrystalline textured structure. The dominant crystalline growth direction is (111). In the case of nickel coating deposited by electrochemical reduction, one of the important parameters affecting the privileged crystallite growth direction is the temperature of the bath from which the coatings are deposited [26]. Widening of reflections on the diffractogram indicates the nanocrystalline structure of the coating. The determined average crystallite size of nickel for the crystallographic direction (111) is 16 nm, and for the direction (200) – 12 nm.

Morphology and surface topography of the Ni/GO composite coatings deposited in the bath with different GO contents are shown in Figures 6-7.

In the case of composite coatings with embedded graphene oxide, there are incompletely enclosed GO agglomerates on the surface, what means that these coatings exhibit a high degree of surface development within convex areas with heights over 150 μm . The incorporation of particles of the dispersing phase occurs simultaneously with the increase of the nickel coating, thanks to which graphene agglomerates encapsulated with nickel can be observed. At the same time as the nickel coating thickness increases, nickel is deposited on the surface of agglomerates of the graphene oxide. The mechanisms of incorporation of the dispersing phase into the metal matrix during the deposition of composite coatings by electrochemical reduction have been described in various ways in a number of works [27,28]. Nevertheless, this phenomenon is not fully understood and depends on many variables, including concentration and type of dispersion phase, mixing speed, cathodic current density, etc. Images of cross-sections of the produced Ni/GO composite coatings are shown in Figure 8.

It is obvious from the above Figure that the composite coatings are characterized by a compact structure and irregular thickness caused by the incorporation of GO flake agglomerates. Diffraction spectra and Raman spectrum of coatings with embedded graphene oxide are shown in Figures 9-10.

The diffraction spectra of Ni/GO composite coatings have reflections corresponding to the nickel matrix material. In the case of Ni/GO composite coatings, the intensity of reflections from the crystallographic direction (200) increases. The nickel matrix crystallites in the Ni/GO composite coatings are the same as for the Ni coating. On the Raman spectrum of the Ni/GO

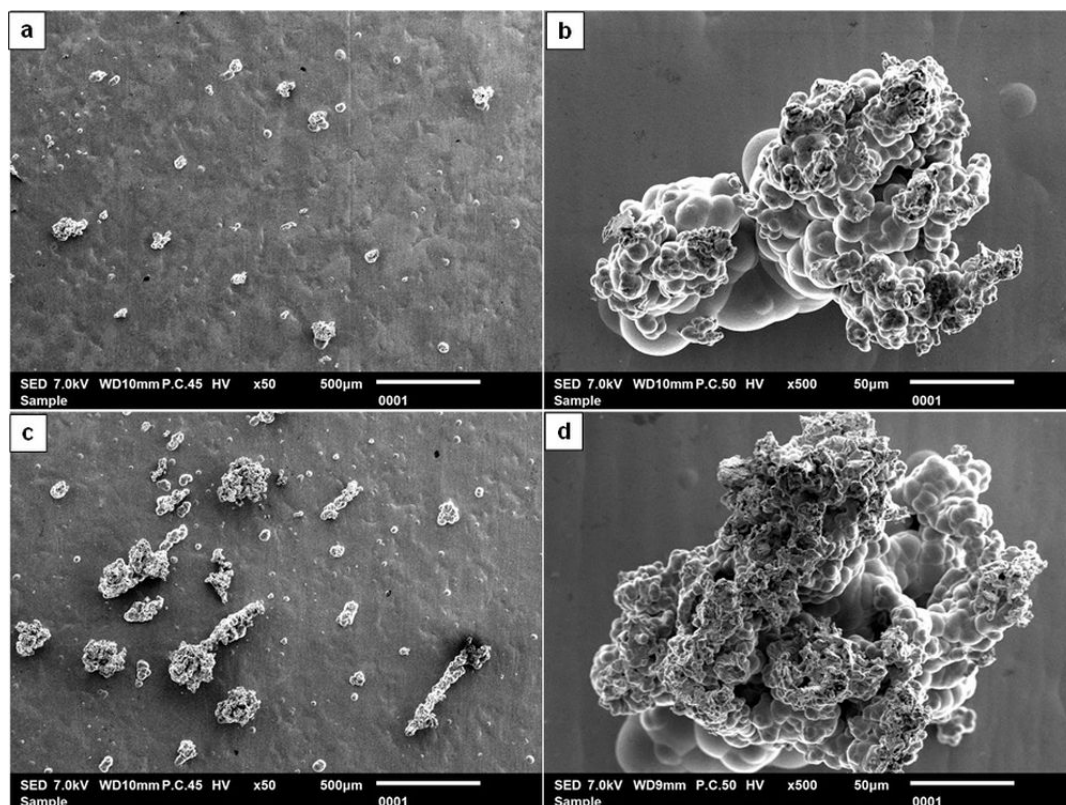


Fig. 6. Surface morphology of Ni/GO (1 ml/dm³) (a, b); Ni/GO (2 ml/dm³) (c, d)

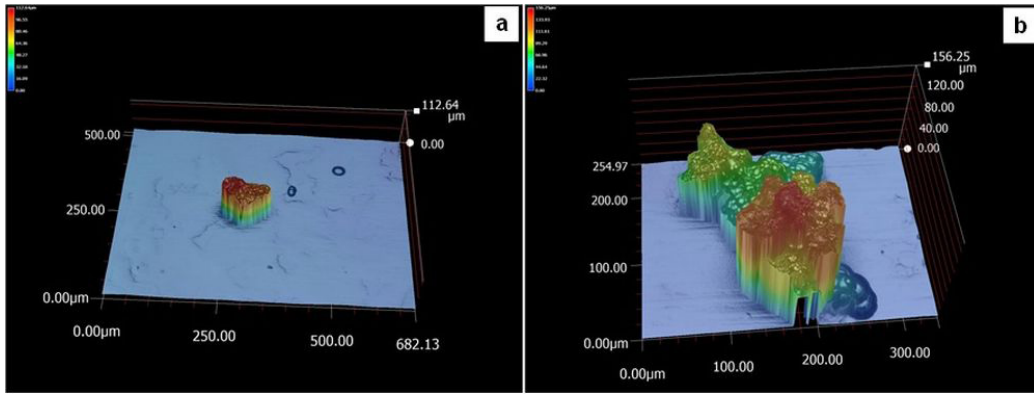


Fig. 7. Topography of coating surfaces Ni/GO (1 ml/dm³) (a); Ni/GO (2 ml/dm³) (b)

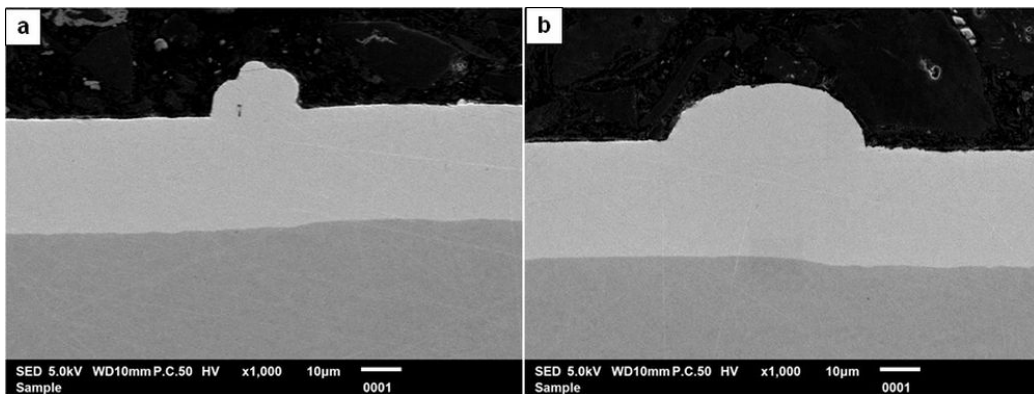


Fig. 8. Cross-sections of the produced coatings: a) Ni/GO (1 ml/dm³); b) Ni/GO (2 ml/dm³)

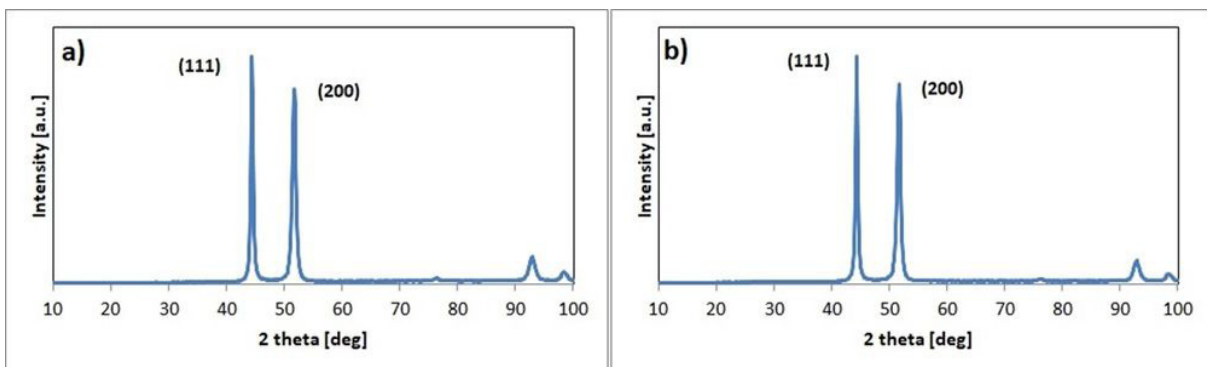


Fig. 9. Diffraction patterns of composite coatings: a) Ni/GO (1 ml/dm³); b) Ni/GO (2 ml/dm³)

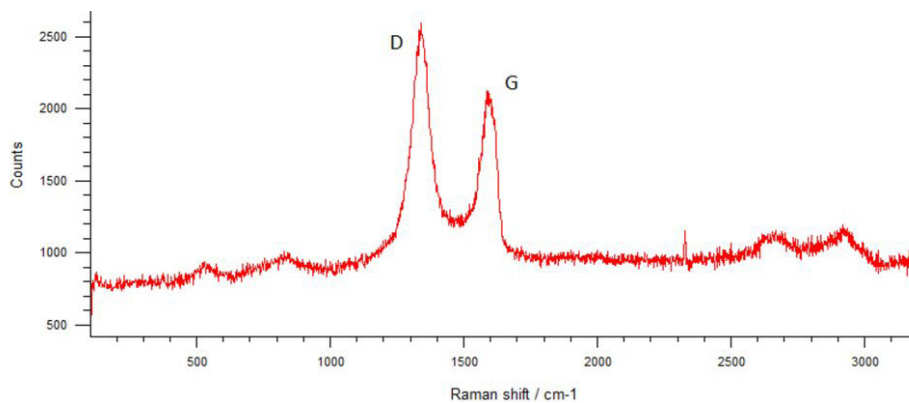


Fig. 10. Raman spectrum of the Ni/GO (2 ml/dm³) coating

composite coating there are two peaks: D (1350 cm^{-1}) and G (1585 cm^{-1}) being characteristic for the graphene oxide. These tests confirm the incorporation of GO into the nickel matrix. Compared with Figure 2, the change in the intensity of the D and G peaks is observed. The determined ratio equals $I_D/I_G = 1.74$ what indicates on a greater disorder of the GO structure embedded in the tested composite material when compared to the pure graphene oxide flakes.

3.3. Coatings properties

Incorporation of graphene oxide flakes into a nickel matrix also affects the properties of the coatings produced by electrochemical reduction method. The results of microhardness measurements HV0.025 of the substrate material and the produced coatings made on cross-sections perpendicular to the sample surface are shown in the graph given in Figure 11.

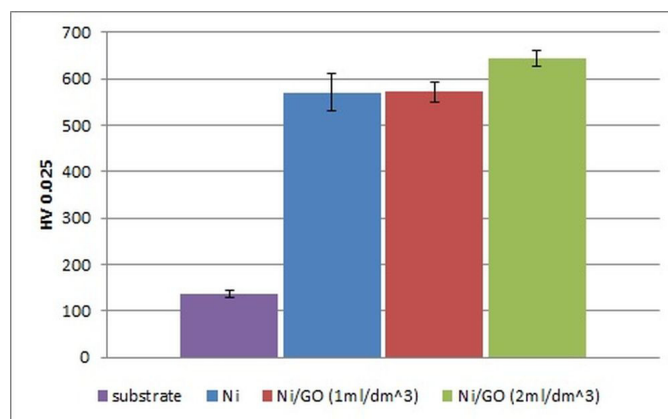


Fig. 11. Microhardness of substrate material, Ni coating and Ni/GO composite coatings

All produced coatings exhibit a higher hardness than a steel substrate. The highest hardness, which is about 650 HV0.025,

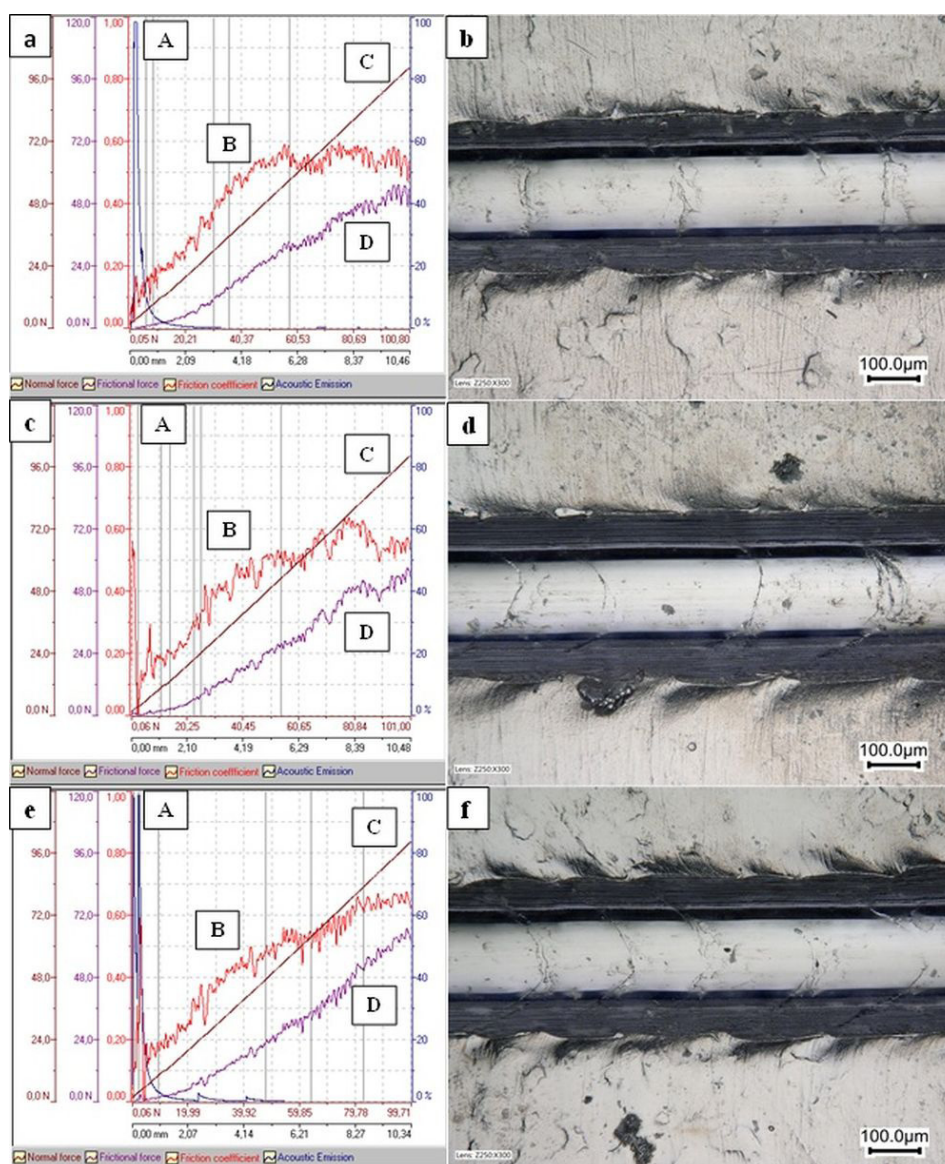


Fig. 12. Graphs of parameter changes during scratch test (A – Acoustic Emission, B – friction coefficient, C – normal force, D – frictional force) and images of scratch fragments: a, b) Ni; c, d) Ni/GO (1 ml/dm³); e, f) Ni/GO (2 ml/dm³)

is demonstrated by coatings deposited in a bath containing 2 ml/dm^3 of an aqueous suspension of graphene oxide. However, the hardness of nickel and composite Ni/GO (1 ml/dm^3) coatings is similar and equal $570 \text{ HV}0.025$. The main mechanisms that may cause strengthening in this type of composite material are: dispersion strengthening (Orowan's mechanism) and strengthening due to the fragmentation of the metal matrix structure in accordance with the dependence of Hall-Petch [29]. The occurrence of these mechanisms results from the introduction of the particles of dispersion phase into the matrix material. According to the Orowan mechanism, the particles introduced into the matrix block the dislocation movement, which in effect leads to strengthening. On the other hand, in accord to the mechanism based on the Hall-Petch relationship, the particles introduced contribute to blocking the growth of crystallites of the metal matrix and the emergence of new crystallization centers. As a result of which increases the share of grain boundaries, which strengthen the material. Unambiguous statement which mechanism in the case is dominant is not possible. No fragmentation of the matrix material structure was found, because the crystallite size for the composite coatings is the same as for the nickel coating. It is also possible to exclude the dispersion strengthening mechanism, which is assumed to be most effective for particles with nanometric dimensions [30]. The graphene oxide used in this study consisted of flakes with micrometric dimensions, however, smaller flakes with diameter well below $1 \mu\text{m}$ could also be present. It is worth mentioning that the quality of coatings used in the engineering applications is largely determined by its adhesion to the substrate. Adhesion of the produced coatings to

the substrate was tested by the scratch method. The results of the scratch tests of Ni and Ni/GO coatings are shown in Figure 12.

The adhesion tests results show that all coatings exhibit a good connection to the substrate. In the images of the damages after the scratch tests (Fig. 14b,d,f), no decohesion of the coatings from the substrate was found. The transverse cohesive cracks occurring in the area of scratch arise as a result of stresses induced before and behind the sliding indenter that moves with increasing pressure force. As a result, plastic and elastic deformations of the coating material occur.

One of the main tasks of coatings is the protection of the substrate material against the corrosive environment. The results of corrosion tests of the substrate material and the coatings

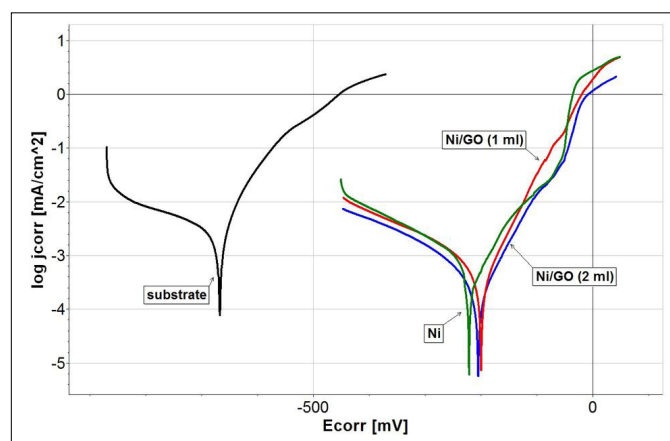


Fig. 13. Potentiodynamic curves of the tested materials in the environment of 0.5 M NaCl

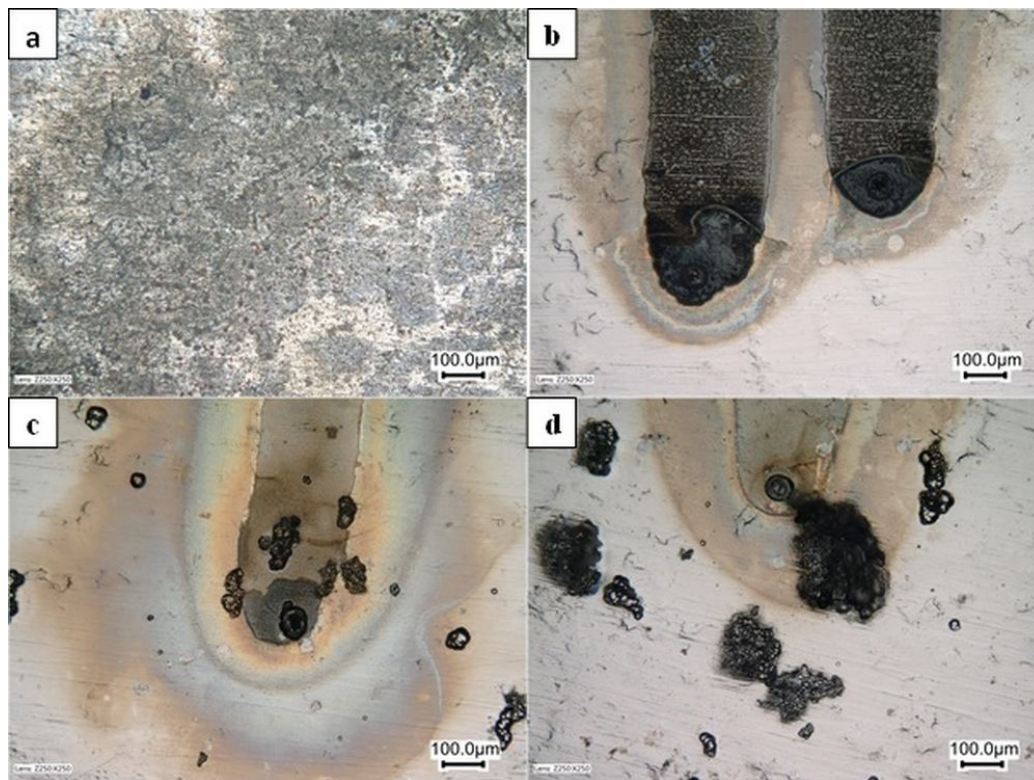


Fig. 14. Images of the steel substrate surface and the coatings surfaces after corrosion tests in 0.5 M solution of NaCl : a) steel; b) Ni; c) Ni/GO (1 ml/dm^3); d) Ni/GO (2 ml/dm^3)

were presented in the form of potentiodynamic curves $j = f(E)$ (Fig. 13). The corrosion potentials E_{corr} and corrosion current densities j_{corr} are presented in Tab. 1.

TABLE 1

Corrosion parameters of the tested materials

Sample	E_{corr} [mV]	j_{corr} [$\mu\text{A}/\text{cm}^2$]
substrate	-667	2.657
Ni	-221	0.860
Ni/GO (1 ml/dm ³)	-198	0.438
Ni/GO (2 ml/dm ³)	-205	0.455

In comparison with a steel substrate, all coatings produced have a significantly higher corrosion resistance under the tested conditions. Differences in the corrosion potential of the produced coatings within 20 mV are not sufficient to allow a clear distinction between the electrochemical behaviour of the tested coatings. However, the corrosion current of composite coatings is two times smaller than that of nickel coating, despite the much higher degree of surface development of composite coatings. The increase in the corrosion resistance of the Ni/GO coatings can be explained by limiting the access of corrosive agents to the matrix through embedded graphene oxide flakes, which constitute a barrier layer [12,31]. Surface of the coatings after corrosion tests are shown in Figure 14. In the case of steel substrates, the damage occurs on the entire exposed surface, while the Ni and Ni/GO coatings exhibit only local damages in the form of pits. Similar results regarding electrochemically deposited Ni coatings were reported in [3,32].

4. Conclusions

Electrochemical reduction of Ni/GO composite coatings in baths with two contents (1 and 2 ml/dm³) of an aqueous suspension of graphene oxide flakes was studied. The incorporation of graphene oxide into a nickel matrix affects the structure, morphology and properties of the produced composite coatings. The increase of GO content in the bath contributes to the increase of the surface development degree, increase of hardness and improves the corrosion resistance of coatings. Composite coatings of Ni/GO are characterized by a compact structure and a good adhesion to steel substrate. Coatings of this type can be used to cover metallic elements in order to improve their functional properties.

REFERENCES

- [1] J. Lapinski, D. Pletcher, F.C. Walsh, Surf. Coat. Tech. **205**, 5205-5209 (2011).
- [2] M. Trzaska, M. Gostomska, Composites Theory and Practice **9**, 84-88 (2009).
- [3] W. Bartoszek et al., Ochrona przed korozją **61**, 36-39 (2018).
- [4] J. Wang et al., Int. J. Refract. Met. H. **70**, 32-38 (2018).
- [5] G.K. Burkat et al., Diam. Relat. Mater. **14**, 1761-1764 (2005).
- [6] M. Trzaska, A. Mazurek, Composites Theory and Practice **16**, 37-41 (2016).
- [7] M. Petrova et al., Arch. Metall. Mater. **61**, 493-498 (2016).
- [8] Z. Karaguiozova et al., Tribology in Industry **39**, 444-451 (2017).
- [9] M. Trzaska, M. Gostomska, Composites Theory and Practice **10**, 133-137 (2010).
- [10] M. Alishahi et al., Appl. Surf. Sci. **258**, 2439-2446 (2012).
- [11] Sung-Kyu Kim et al., Trans. Nonferrous Met. Soc. China **21**, 68-72 (2011).
- [12] A. Gajewska-Midziątek, Pol. J. Chem. Tech. **20**, 54-59 (2018).
- [13] G. Cieślak, M. Trzaska, Pol. J. Chem. Tech. **20**, 29-34 (2018).
- [14] C. Liu et al., Appl. Surf. Sci. **351**, 889-896 (2015).
- [15] H. Wu et al., Surf. Coat. Tech. **272**, 25-32 (2015).
- [16] M.Y. Rekha et al., Thin Solid Films **636**, 593-601 (2017).
- [17] M.H. Sathir et al., Appl. Surf. Sci. **320**, 171-176 (2014).
- [18] H. Algul et al., Appl. Surf. Sci. **359**, 340-348 (2015).
- [19] B. Szczygieł, M. Kołodziej, Electrochim. Acta **50**, 4188-4195 (2005).
- [20] A. Kozik et al., Arch. Metall. Mater. **61**, 375-380 (2016).
- [21] N.P. Wasekar et al., Surf. Coat. Tech. **291**, 130-140 (2016).
- [22] <https://graphene-supermarket.com/Dispersion-in-Water-Single-Layer-Graphene-Oxide-175-ml.html>
- [23] Y. Raghupathy et al., Thin Solid Films **636**, 107-115 (2017).
- [24] W. Konicki, M. Aleksandrak, E. Mijowska, Pol. J. Chem. Tech. **19**, 120-129 (2017).
- [25] M. Trzaska, A. Mazurek, Ochrona przed Korozją **58**, 404-406 (2015).
- [26] J. Abdul et al., RSC Adv. **7**, 31100-31109 (2017).
- [27] A. Hovestad, L.J.J. Janssen, J. Appl. Electrochem. **25**, 519-527 (1995).
- [28] E. Łągiewka, A. Budniok, Struktura, właściwości i metody badań materiałów otrzymanych elektrolitycznie, Katowice 2010.
- [29] F. Hou et al., Appl. Surf. Sci. **252**, 3812-3817 (2006).
- [30] Z. Zhang, D.L. Chen, Scripta Mater. **54**, 1321-1326 (2006).
- [31] M. Sajjadnejad et al., J. Alloy. Compd. **704**, 809-817 (2017).
- [32] G. Cieślak, M. Trzaska, Ochrona przed Korozją **61**, 70-73 (2018).